17
Microstructured Reactors for Electrochemical Synthesis*

Sabine Rode and François Lapicque

Electrochemistry is an extremely diversified field describing any kind of system where a chemical reaction takes place at an electrified interface and is coupled with an electron transfer between an electronic and an ionic conductor. Well-known application fields are electroanalytical devices, electrowinning of metals, electroplating, energy storage in batteries, energy conversion in fuel cells and the synthesis of a great variety of inorganic and organic compounds. The electrochemical reactors used in these different application fields are various and it is outwith the scope of this chapter to discuss the impact of microstructuring on all of them. Instead, this chapter focuses on a particular application field: electrochemical synthesis. Moreover, the reactor layout is analyzed from the point of view of process engineering whereas electrocatalytic aspects, even though extremely important in electrochemical engineering, are not treated.

In the first section, some fundamentals of electrochemical processes are defined. Common industrially relevant process flow schemes and equipment are described in the second section. The third section discusses the interest of microstructured reactors in electrochemical synthesis and gives an overview of the recent literature in this area.

17.1
Fundamentals of Electrochemical Processes

Fundamentals of electrochemical processes can be found in several textbooks [1–5]. The electrochemical reactor is an electrolytic cell, shown schematically in Figure 17.1, powered by a current source. The cell contains positively charged anodes and negatively charged cathodes in addition to an electrolyte solution containing ions which permit to carry the electric current through the solution. The reactant and the products are usually at least partially dissolved in the electrolyte.

*A List of Symbols can be found at the end of this chapter.

Micro Process Engineering, Vol.1: Fundamentals, Operations and Catalysts
Edited by V. Hessel, A. Renken, J.C. Schouten, and J.-I. Yoshida

ISBN: 978-3-527-31550-5

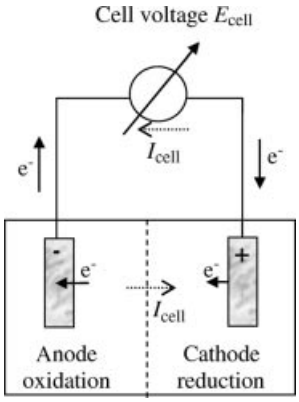

Figure 17.1 Schematic view of an electrochemical cell.

The anodic and the cathodic half-cells may be separated by a membrane or a porous diaphragm.

17.1.1
Electrode Reaction Stoichiometries and Faraday's Law

Electrochemical reactions are heterogeneous reactions characterized by at least one electron charge-transfer step. The electron e^-appears thus in the reaction equation with its stoichiometric coefficient n. The anodic oxidation of a reagent A to form the product B can be written as

$$A \rightarrow B + ne^- \tag{17.1}$$

and the cathodic reduction of reagent C to form reagent D can be expressed as

$$C + n'e^- \rightarrow D \tag{17.2}$$

where n' is a stoichiometric coefficient. Electrochemistry is only possible in a cell which contains both an anode and a cathode and, owing to the need to maintain an overall charge balance, the amount of electrons exchanged in the reduction at the cathode and in the oxidation at the anode must be equal. The total chemical change in the cell is determined by adding the two individual electrode reactions:

$$A + \frac{n}{n'}C \rightarrow B + \frac{n}{n'}D \tag{17.3}$$

The relations established in the following are developed on the example of Equation (17.1) for the anodic half-cell reaction or Equation (17.3) for the overall cell reaction.

The electric charge required to convert 1 mol of reagent in a reaction involving n electrons per mole is given by Faraday's law of electrolysis:

$$Q_{mol} = nF \tag{17.4}$$

17.1.2
Electrode Potentials and Gibbs Free Energy Change of the Overall Reaction

The equilibrium potential of an electrochemical reaction is defined as the potential of an electrode (with respect to the potential of a normal hydrogen electrode) when immersed in an electrolytic cell containing the reactive species, but without current flow. When a current is applied, the electrode potential is shifted. In the case of an anodic reaction:

$$E^{a} = E_{e}^{a} + \eta^{a} \tag{17.5}$$

where E^{a} is the anodic potential, E_{e}^{a} the equilibrium potential of the anodic reaction and η^{a} the anodic overpotential, which is linked to the charge-transfer rate. The cathodic potential is defined in an analogous manner:

$$E^{c} = E_{e}^{c} + \eta^{c} \tag{17.6}$$

The difference between the equilibrium potentials of the half-cell reactions $E_{e}^{c} - E_{e}^{a}$ is related to the Gibbs free energy change ΔG of the overall cell reaction is

$$\Delta G = \Delta H - T\Delta S = -nF\left(E_{e}^{c} - E_{e}^{a}\right) \tag{17.7}$$

where ΔH and ΔS are the enthalpy and the entropy change, respectively, of the overall cell reaction, which are defined and calculated as in classical chemical reactions. Electrochemical synthesis is concerned with carrying out reactions where the free energy change is positive, i.e. $E_{e}^{c} - E_{e}^{a}$ is negative. Electrolytic methods may even be used to drive very unfavorable reactions.

17.1.3
Kinetics and Mass Transfer Limitations of the Electrode Reaction

The overpotential terms of Equations (17.5) and (17.6) are the driving forces of the electrochemical reaction. The most commonly used kinetic expression in electrochemistry is undoubtedly the Tafel law, which predicts an exponential increase of the current density of the desired reaction, i_{A}, with the electrode overpotential. For the anodic reaction of Equation (17.1):

$$i_{A} = nFk_{A}C_{A}^{i}\exp(b_{A}\eta^{a}) \tag{17.8}$$

where k_{A} and b_{A} are kinetic constants which depend strongly on the electrode material and on the electrolyte composition and temperature. C_{A}^{i} is the reagent concentration at the electrode surface.

Under steady-state conditions, the reagent flux from the bulk to the electrode surface, frequently modeled by a Newton-type law, equals the reagent consumption due to the electrochemical reaction:

$$k_{m}\left(C_{A}^{b} - C_{A}^{i}\right) = \frac{i_{A}}{nF} \tag{17.9}$$

where C_A^b is the reagent concentration in the bulk. Combination of Equations (17.8) and (17.9) permits the removal of the interfacial reagent concentration:

$$i_A = \frac{nFk_m C_A^b}{1 + \frac{k_m}{k_A}\exp(-b_A \eta^a)} \tag{17.10}$$

For high anodic overpotentials, a limiting current density, corresponding to the maximum possible mass transfer, is obtained:

$$i_{A\,lim} = nFk_m C_A^b \tag{17.11}$$

Due to economic factors, large-scale processes are generally driven close to the transport-limited rate [2].

17.1.4 Process Performance Criteria

In order to evaluate and to compare different process options, performance criteria or "figures of merit" have been developed in the domain of electrochemical process engineering. For the reaction described in Equation (17.1) performed in a continuous flow reactor in steady-state flow, the reagent conversion θ, product selectivity σ and material yield ψ are defined by

$$\theta = \frac{\dot{n}_A^{in} - \dot{n}_A^{out}}{\dot{n}_A^{in}} \tag{17.12}$$

$$\sigma = \frac{\dot{n}_B^{out}}{\dot{n}_A^{in} - \dot{n}_A^{out}} \tag{17.13}$$

$$\psi = \frac{\dot{n}_B^{out}}{\dot{n}_A^{in}} \tag{17.14}$$

where $\dot{n}$ is a molar flux. These definitions are those found in classical chemical engineering and, as in the latter, high conversions and selectivities are desired. In electrochemical processes, an additional performance parameter appears, namely the current efficiency, defined as the yield based on the electrical current passed during the electrolysis:

$$\Phi = \frac{nF\dot{n}_B^{out}}{I} \tag{17.15}$$

Current efficiencies below unity indicate either that to some extent the back reaction occurs on the counter-electrode, or, more likely, that undesired products are being formed. These may, however, arise by electrolysis of the solvent or the carrying electrolyte. Hence they are not necessarily associated with a material yield lower than unity.

One of the most valuable statements of reactor performance is the space–time yield, which expresses the mass amount of product per unit of time and reactor volume V_R:

$$\rho_{st} = \frac{M_B \dot{n}_B^{out}}{V_R} = \frac{M_B \Phi I}{nFV_R} = \frac{M_B \Phi \bar{i}\, a_s}{nF} \tag{17.16}$$

where M_B is the molar mass of the product, $\bar{i}$ the average current density applied in the cell and a_s the specific electrode area, i.e. the electrode area per reactor volume. In commercial processes, the average current density applied is typically on the order of magnitude of the limiting current density of the reagent [Equation (17.11)] and the space–time yield is proportional to the following terms:

$$\rho_{st} \approx \frac{M_B \overline{i_{A\,lim}} a_s}{nF} = k_m M_B \overline{C_A^b} a_s \tag{17.17}$$

It is therefore an important challenge to electrochemical engineers to design electrolytic cells characterized by high mass transfer coefficients and important specific electrode area.

17.1.5
Specific Energy Consumption and Cell Voltage

The specific energy consumption states the electric power required to make unit weight of the product. It is a function of both the electrolysis conditions and the cell design. The specific energy consumption is given by [2]

$$\text{Specific energy consumption} = \frac{-nFE_{cell}}{\Phi M_B} \tag{17.18}$$

where E_{cell} is the cell voltage which has a negative value in electrochemical cells which are not power generators, which is the case of electrosynthesis applications. The specific energy consumption is a function of the cell voltage and of the current efficiency. Hence it can be minimized only by selecting electrolysis conditions that lead to high current efficiencies and to absolute values of the cell voltage as low as possible.

The cell voltage is a complex quantity which depends on the electrode potentials [Equations (17.5) and (17.6)], but also on the ohmic potential drops IR, which are related to the current flow through the electrochemical cell and the electric circuit (cables, current leads, etc.):

$$E_{cell} = E_e^c - E_e^a - |\eta^c| - |\eta^a| - IR_{cell} - IR_{circuit} \tag{17.19}$$

Whereas the cell voltage is a global parameter, the electrode potentials and the ohmic drops are local parameters which are, of course, interdependent.

17.1.6
Ohmic Drop and Heat Generation

The ohmic drop in the electrochemical cell is related to the potential field in the electrolyte, which depends on the geometry and the arrangement of electrodes and

also on the voltage applied between the electrodes and on the electrolyte conductivity. For parallel electrodes with a uniform current density distribution, the ohmic drop is distributed uniformly and can be expressed by Ohm's law:

$$IR_{\text{cell}} = \Delta\Phi_{\text{ohm}} = \frac{\bar{i}\, d}{\kappa} \tag{17.20}$$

where d is the inter-electrode gap and κ the electrolyte conductivity.

Heat is generated in the electrochemical cell by means of electrical power loss related to the cell voltage, referred to as Joule heating, and also mechanical power loss related to the electrolyte flow. The Joule heating of the system is given by [2]

$$Q_{\text{Joule}} = I(E_{\text{cell}} - E_{\text{tn}}) \tag{17.21}$$

where E_{tn} is the thermoneutral voltage of the cell, defined by

$$E_{\text{tn}} = -\frac{\Delta H}{nF} \tag{17.22}$$

The ohmic drop frequently represents an important fraction of the cell voltage and plays a major role in the heat generation terms. This is especially true in organic electrosynthesis where current densities are high and electrolyte conductivities low. *A major concern in electrochemical engineering is clearly linked to the design of cells with minimum ohmic drops.*

17.2 Electrochemical Equipment and Process Flow Schemes

The diversity of electrosynthesis reactions and reactors is tremendous and it is clearly outwith the scope of this chapter to deal with all of them. After the definition of important fundamental process options, the geometry of the most common commercial cells is briefly described and typical overall process flow schemes are discussed.

17.2.1 Some Overall Process Options

17.2.1.1 Divided and Undivided Cells

As mentioned in Section 17.1, the anodic and cathodic compartments of an electrochemical cell can be separated by an ion-exchange membrane or a porous diaphragm. The division of a cell is often practiced in industrial processes, despite the additional costs, the need for additional seals and possible maintenance problems. A separator may indeed allow a more independent choice of anode/anolyte or cathode/catholyte, enable current efficiency to be maintained due to the exclusion of redox shuttles and help to isolate electrode products or prevent the formation of explosive or toxic mixtures, for example H_2–O_2. However, if possible, undivided cells are preferred, as they lead to lower ohmic drops and to much simpler technologies.

17.2.1.2 Direct and Indirect Electrosynthesis

In direct electrosynthesis, the desired product is formed by means of an electrochemical reaction. In indirect electrosynthesis, a redox couple is used as an "electron carrier" for the oxidation or reduction of another species in the system. In other words, the electrode is used to reconvert the redox reagent continuously to an oxidation state where it is able to react with another compound in a desirable, generally homogeneous redox reaction. Most suitable redox couples are inorganic whereas the desired product is typically organic. The final redox step may be carried out inside or outside the electrochemical cell.

17.2.1.3 Simple and Paired Electrosynthesis

As discussed in Section 17.1.1, electrochemical cells always involve two electrochemical reactions, anodic and cathodic. Currently, only one of the products is valuable whereas the other is a valueless side product. A common case is the anodic oxidation of an organic substrate combined with the cathodic production of hydrogen. Some processes, however, permit "paired electrosynthesis" characterized by the simultaneous formation of valuable products at both electrodes. This combination, if possible, is extremely interesting as it allows waste to be minimized. Paired electrosynthesis reactions can be parallel (two reagents give two products), divergent (one reagent gives two products) or convergent (two reagents give a single final product). In the last case, a homogeneous reaction step permits the combination of the intermediates formed by the heterogeneous electrode reactions.

17.2.2 Typical Commercial Cells

An overview of the various types of electrochemical cells that are of importance for industrial electrosynthesis processes is given in several textbooks [1–5]. Only the main cell types are briefly discussed here. Despite the diversity of cell design, there are clearly some general rules [2]. The achievement of a correct rate and selectivity of production requires control and uniformity of the mass transfer rate and also of the potential and current distribution. This is best attained by a parallel electrode configuration, leading to a constant inter-electrode gap and thus, it is expected, to a uniform potential field. The control and minimization of the inter-electrode gap are particularly important in direct electrosynthesis, where high reagent concentrations and high current densities are desirable.

17.2.2.1 Tank Cells

The tank cell is the classical batch or semi-batch reactor of electrochemical technology. In most tank cells, the electrodes are vertical and made from sheet, gauze or expanded material. The cell is arranged with parallel lines of alternate anodes and cathodes, the electrodes extending across and to the full depth of the tank. The anode–cathode gap is made as small as possible to maximize the space–time yield and to reduce the energy consumption. It is unusual in tank cells to induce convection by mechanical means, but electrolyte stirring is in generally promoted

by gas bubbles evolving at the electrodes. The great advantage of the tank cell is the simplicity of construction and the wide range of materials which can be used for its manufacture. It is, however, poorly suited to large-scale operation or to a process where control of the mass transfer rate is required.

17.2.2.2 Filterpress-type Flow Cells

The majority of commercial electrochemical reactors have up to now been flow cells involving parallel electrodes disposed in a plate-and-frame arrangement and mounted on a filterpress [2, 4]. The mass transfer rate is promoted in these cells by high electrolyte velocities obtained through external electrolyte pumping and eventually turbulence promoters such as plastic meshes. The electrodes are generally disposed vertically in order to facilitate gas evolution. Separators can be introduced if the cathodic and the anodic compartments are to be divided. In plate-and-frame cells, it is normal to reduce the inter-electrode gap to 0.5–5 cm. Although the potential distribution in a parallel-plate cell is good and the mixing conditions can be made to meet most requirements, it is often difficult to reduce the inter-electrode gap sufficiently to obtain the desired space–time yield and energy efficiency [2].

17.2.2.3 Cells with Parallel Electrodes and a Millimeter or Submillimeter Inter-electrode Gap

The minimization of the anode–cathode gap is clearly recognized to be an important process parameter, especially in electro-organic synthesis where electrolyte conductivities are low and where the ohmic drop is a major concern. Two undivided electrochemical cells leading to the minimization of the inter-electrode gap are commercially exploited. In the Swiss-roll cell shown schematically in Figure 17.2a, thin metal foils are separated by a plastic mesh and wrapped around a central core. The electrolyte flows axially through the cell and mass transfer is promoted by the mesh. The inter-electrode gap is typically small (0.2–2 mm) [2], providing a low cell voltage and promoting uniform flow and electrode potential distributions. The design is cartridge oriented and electrode or separator changes are made via a

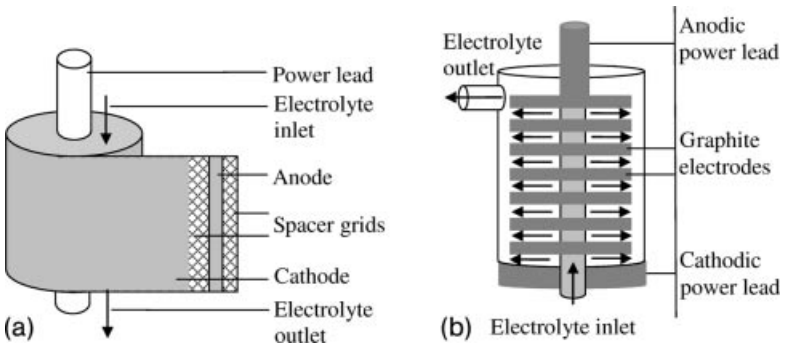

Figure 17.2 Schematic view of undivided electrochemical cells with a small inter-electrode gap. (a) Swiss-roll cell; (b) capillary gap cell.

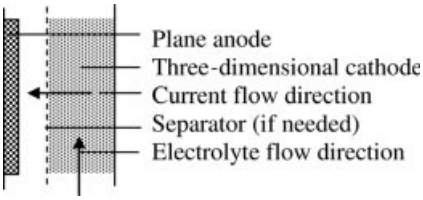

Figure 17.3 Schematic view of an electrochemical cell with a three-dimensional flow-through electrode arrangement.

replacement module. The technology is, however, restricted to undivided cells and to metal electrodes. Carbon electrodes are used in the capillary-gap cell, shown schematically in Figure 17.2b, which consists of circular graphite disks kept apart by insulating spacers. The electrolyte enters via a central channel and flows radially between the disks. The inter-electrode gap is in the millimeter range (1–2 mm).

17.2.2.4 Cells with Non-parallel Dissymmetric Electrodes

In cases of low concentrations of the electroactive species, as typically observed in metal recovery but also in indirect electrolysis processes, the specific electrode area and also the mass transfer coefficient must be maximized in order to reach a reasonable space–time yield [Equation (17.17)]. This can be obtained using three-dimensional electrodes. In this configuration, as illustrated schematically in Figure 17.3, the electrolyte flows through a by some means porous electrode. Electrochemical cells with porous electrodes are characterized by non-constant, relatively important anode–cathode distances. They are suitable for processes involving low current densities and high electrolyte conductivities. However, porous electrodes commonly lead to non-uniform electrode potentials and, hence, to a non-uniform current distribution within the bed, along with the dimension parallel to the current flow. These geometries are poorly suited to direct electro-organic synthesis purposes, where current densities are high and electrolyte conductivities are low.

17.2.3 Process Flow Schemes

The economy of electrolytic processes, especially in the synthesis of organic specialties, is closely related not only to the electrochemical cell, but also to the straightforwardness of product purification [1]. This means that the main objective for the successful development of a new product from organic electrochemistry is closely related to the best process flow scheme, combining the different process steps.

Electrochemical flow cells commonly suffer from the problem that the conversion per pass is low. For this reason, it is common to run such cells with an electrolyte reservoir and to recirculate the electrolyte repeatedly through a cell or group of cells and back to the reservoir. If the electrochemical process including the flow cell is operated batchwise, it is known as a batch recycle process (Figure 17.4a). The reagent concentration in the reservoir decreases with time and the process is stopped when

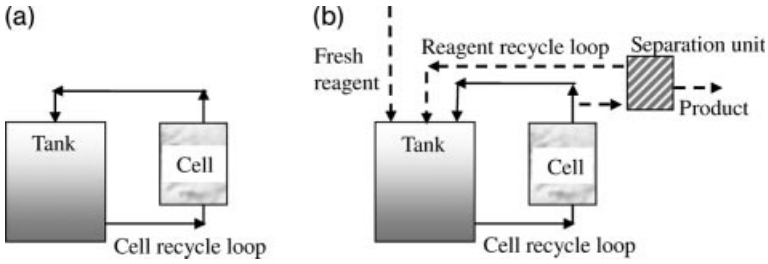

Figure 17.4 Production schemes for organic electrosynthesis. (a) Batch recycle process; (b) continuous process including reagent recycle.

the desired conversion is reached. Although the current distribution is ideally spatially uniform within the electrochemical reactor, the applied current density must be lowered with time, in order to adjust to the decreasing reagent concentration and to avoid undesired side reactions. Another disadvantage of this scheme is the batch mode of operation, which is poorly suited to high production rates.

The electrochemical process including the low-conversion flow cell and the recycle loop can also be operated in a continuous manner (Figure 17.4b). In this case, fresh reagent is continuously fed to the reservoir and a fraction of the electrolyte is continuously withdrawn. The reagent and the product are separated to concentrate the product and to recycle the reagent. In order to work at high current density and thus at a high productivity, the reagent concentration in the loop and thus in the electrolyte tank should be as high as possible. Major disadvantages of this scheme are the complexity of the recycle loops and the relatively large size of the separation unit.

17.3 Microreactors in Electrochemical Synthesis

The development of microtechniques permits electrochemical synthesis reactors to be conceived that are characterized by electrodes and/or inter-electrode gaps in the sub-millimeter range. Even though some commercial cells already approach sub-millimeter inter-electrode gaps (see Section 17.2.2.3), microtechnologies permit us to go further, and gaps of less than 0.2 mm are attained [6–12], various electrode materials can be considered [6] and electrode segmentation or heat exchangers may be integrated in the reactor design [6, 13]. The sub-millimeter electrode widths and/or inter-electrode gaps lead to the quantitative but also to the qualitative variation of several process parameters, resulting in process intensification. The most important mechanisms of process intensification via microstructuring are outlined in Section 17.3.1. The subsequent sections describe in more detail the two types of microstructured reactors investigated in the recent literature, i.e. coplanar interdigitated band electrodes, treated in Section 17.3.2, and microplate or microchannel reactors, discussed in Section 17.3.3.

17.3.1 Process Intensification Mechanisms

17.3.1.1 Enhancement of the Mass Transfer Rates

Sub-millimeter inter-electrode gaps (in the case of plate and channel reactors) or electrode widths (in the case of coplanar interdigitated band electrodes) lead to thin concentration boundary layers with any flow rate [14, 23] resulting in enhanced mass transfer rates and thus increasing the attainable space–time-yield [Equation (17.17)].

17.3.1.2 Coupling of the Electrode Processes

The decrease in the inter-electrode gap may lead to the overlapping of the anodic and cathodic diffusion layers [7–11, 17–19]. This is referred to as "coupling" of the electrode processes. Charged reaction intermediates, often protons or hydroxide ions produced by the electrode reactions, accumulate in the diffusion boundary layers and act as electrolyte. *The coupling of the electrode processes thus increases the conductivity in the inter-electrode gap*. The coupling of the electrode processes confers a particular advantage in the case of paired convergent electrosynthesis reactions (see Section 17.2.1.3 for the definition), as it accelerates the final homogeneous reaction step by facilitating the mass transfer between the electrogenerated intermediates [16,18, 20].

17.3.1.3 Reduction of the Ohmic Drop

As illustrated in Equation (17.20) for parallel electrodes and a uniform current distribution, the ohmic drop decreases with decrease in the inter-electrode gap and with increase in the electrolyte conductivity. *In microstructured reactors, the small inter-electrode gap together with the conductivity increase due to the coupling of the electrode processes leads to a substantial reduction in the ohmic penalty* [7, 8]. Hence microstructured designs permit one to minimize the cell voltage [Equation (17.19)], the specific energy consumption of the electrochemical cell [Equation (17.18)] and the heat generation terms [Equation (17.21)].

The low ohmic drop reduces the need for supporting electrolyte. Several research teams have shown that it is even possible to work without the addition of a conducting salt [7–11]; the resulting processes are referred to as "self-supported". The absence of a conducting salt reduces costs since it has neither to be purchased nor removed from the reaction mixture.

17.3.1.4 Operation in Single-pass High-conversion Mode

In microplate and microchannel reactors, the electrolyte flows between the plane electrodes and the small inter-electrode gap leads to a high surface-to-volume ratio, i.e. a high specific surface area. *High specific electrode areas not only increase the space–time yield of the reaction [*Equation (17.17)*], but also permit electrosynthesis reactions to be performed in a single-pass high-conversion mode, leading to a continuous process without recycle* [7–12]. This process scheme has two major advantages over the classical process flow schemes described in Section 17.2.3: it requires only a small separation unit and both the short residence time and the plug flow of the reagent, minimize undesired side reactions.

17.3.2
Coplanar Interdigitated Microband Electrodes

Girault and co-workers [14–19] developed the concept of coplanar interdigitated microband electrodes illustrated schematically in Figure 17.5 The electrodes are built by successive screen printing of conductive and insulating layers on a substrate (stainless steel or aluminum). Various electrode materials such as platinum and ruthenium oxide are employed. Electrode widths are in the range 0.5–1 mm, with a gap between the electrodes varying from 0.25 to 1 mm. For most investigations, the electrode band length is between 20 and 27 mm and the total number of bands on a plate is between 20 and 70. Syntheses are carried out in a 150 mL tank reactor and also in a flow cell characterized by a flow section 4 mm in depth and 20 mm in width [15–17, 19].

Two indirect organic electrosynthesis reactions have been investigated: the methoxylation of furan in methanol [15] and the epoxidation of propylene in water [16]. The anodic redox couple for the two systems is bromide–bromine (Br^-–Br_2), whereas the cathodic reaction results in hydrogen formation. The authors emphasize the low energy consumption associated with the low ohmic drop, but also the good performance of the interdigitated system in terms of mass transfer. The latter is due to the periodic relaxation of the mass transfer boundary layer. Good mass transfer coefficients are obtained even without convective electrolyte flow and the authors suggest the use of the technology in tank reactors in order to increase the mass transfer rates. The epoxidation of propylene is a paired convergent electrolysis system, as the hydroxide ions resulting from the cathodic reaction allow the formation of the propylene oxide which is the final product. Belmont and Girault underline the fact that the coupling of the electrode processes facilitates the overall reaction [16].

Girault and co-workers reported the application of plane interdigitated microband electrodes to an inorganic electrosynthesis of industrial interest: the hypochlorite generation from sea water electrolysis. The system was studied in a laboratory cell [17] and also in a pilot plant [19]. A major problem in this synthesis is related to the deposition of scale (calcium and magnesium hydroxide) on the cathode due to the local production of OH^- anions. The coupling of the electrode processes permits the pH excursions on the cathode to be restricted, leading to a decrease in scale deposition.

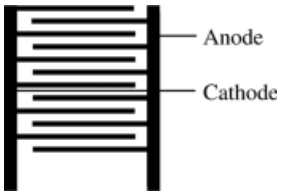

Figure 17.5 Schematic representation of the coplanar interdigitated electrode band geometry.

The major drawback of the technology of coplanar interdigitated microband electrodes is related to the fabrication technique: the electrode materials are restricted to those that can be screen-printed and the voltage drop in the thin layer electrodes can be important, leading to non uniform overvoltage and current distributions [19]. Finally, the specific electrode areas developed by the interdigitated design are smaller than those developed with simple plane electrodes.

17.3.3 Plate and Channel Microreactors

A straightforward manner to apply microtechniques to electrochemical synthesis reactors is to develop parallel plate reactors with a sub-millimeter inter electrode gap. The plane electrodes are separated by isolating spacers, which may lead to the formation of parallel flow channels. In any case, the electrodes are plane sheets which can be replaced and thus made out of any plain material, e.g. nickel, lead, glassy carbon or graphite. *Recent technological developments made at the Institute of Microtechniques, Mainz* [6, 7]*, have led to the construction of versatile microchannel electrochemical reactors.* Indeed, the pressure can be elevated to up to 35 bar and the electrodes can be stacked in order to increase the overall electrode area. Moreover, polymer electrolyte membranes can be inserted, separating anodic and cathodic compartments if necessary, and finally heat exchangers may be integrated.

A major interest of micro-scale plate and channel reactors is related to the high specific electrode area, permitting operation in a single-pass high-conversion mode. This mode is characterized by some special features which are detailed in Sections 17.3.3.1–17.3.3.4. The subsequent sections discuss the experimental and theoretical investigations reported in the recent literature.

17.3.3.1 Reagent Flux and Applied Current

A dimensionless current, comparing the applied electrical current to the current necessary to entirely convert the reagent flux, can be defined:

$$I^* = \frac{I}{nF\dot{n}_A^{in}} = \frac{I}{nFC_A^{in}Q_L} = \frac{\Psi}{\Phi} \tag{17.23}$$

A single-pass high-conversion electrochemical cell should ideally operate at a dimensionless current close to unity, permitting high yields to be obtained at high current efficiencies. *Dimensionless currents higher than unity are not desirable in principle as they are always associated with current efficiencies lower than unity.* Furthermore, if the secondary reactions involve the desired product, dimensionless currents higher than unity lead to a rapid decrease in the material yield.

17.3.3.2 Mass Transfer Limitations and Reagent Conversion

Due to the important ratio between the reactor length and the inter-electrode distance, plate and channel microreactors behave like plug flow reactors. The maximum possible conversion is reached if the reaction is under mass transport control on the entire electrode surface. The combination of the local diffusion-limited

current density [Equation (17.11)] and the material balance on a reactor slice (assuming a constant electrolyte velocity) leads to

$$\frac{dC_A(x)}{dx} = -\frac{i_{A\,lim}(x)}{nFu_L d} = -\frac{k_m C_A(x)}{u_L d} \tag{17.24}$$

where u_L is the superficial electrolyte velocity. The integration of Equation (17.24) over the electrode length L permits the determination of the maximum possible reagent conversion:

$$\theta = \frac{C_A^{in} - C_A^{out}}{C_A^{in}} = 1 - \exp\left(-\frac{k_m L}{u_L d}\right) \tag{17.25}$$

The dimensionless number appearing in the exponential factor in Equation (17.25) is the number of transfer units (*NTU*), as it compares a characteristic mass transfer flux, $k_m\Omega$, with the overall flux Q_L:

$$NTU = \frac{k_m L}{u_L d}\frac{w}{w} = \frac{k_m \Omega}{Q_L} \tag{17.26}$$

where w is the electrode width, Ω the electrode surface area and Q_L the volumetric electrolyte flow rate. Equation (17.25) *demonstrates that single-pass high-conversion microreactors imply high NTU values*. For example the *NTU* necessary to obtain, under mass transfer control, a conversion of 99% is 4.6. If the reactor works beyond the limiting current density, the *NTU* necessary for high conversion is even higher.

17.3.3.3 Liquid–Solid Mass Transfer Coefficient and Coupling of the Electrode Processes

In a small-gap parallel-plate reactor with laminar liquid flow (without gas evolution), infinitely wide electrodes and a constant electrode surface concentration, the average Sherwood number over the electrode length is given by Lévêque's equation [21]:

$$\overline{Sh} = \frac{\overline{k_m} d}{D} = 1.85\left(ReSc\frac{d}{L}\right)^{\frac{1}{3}} = 1.85\left(\frac{DL}{u_L d^2}\right)^{-\frac{1}{3}} \tag{17.27}$$

Equation (17.27) describes a developing mass transfer boundary layer in a fully-developed laminar flow. However, if the mass transfer boundary spans the whole electrode gap, the Sherwood number attains a limiting value which is independent of flow hydrodynamics. The limiting Sherwood number is given, for a uniform mass flux at the electrode surface by [21]

$$Sh_{lim} = \frac{k_m d}{D} = 2.69 \tag{17.28}$$

Equation (17.28) holds if the mass transfer boundary layer is fully developed, which is verified for the following condition (see [22] for the case of the heat transfer boundary layer):

$$\frac{DL}{u_L d^2} > 0.1 \tag{17.29}$$

The combination of Equation (17.27) or (17.28) with the definition of *NTU* [Equation (17.26)] permits *NTU* to be expressed in the case of a non-developed [Equation (17.30)] or a developed [Equation (17.31)] concentration profile.

$$\frac{DL}{u_L d^2} < 0.1 \quad NTU = 1.85\left(\frac{DL}{u_L d^2}\right)^{\frac{2}{3}} \tag{17.30}$$

$$\frac{DL}{u_L d^2} > 0.1 \quad NTU = 2.69\frac{DL}{u_L d^2} \tag{17.31}$$

Equations (17.30) and (17.31) demonstrate that single-pass high-conversion microreactors which are characterized by NTU higher than unity (see Section 17.3.3.2) imply fully developed mass transfer boundary layers for the major part of the electrode surface. The electrode processes are thus coupled. The mass transfer coefficient is independent of the liquid phase flow rate and can be estimated using Equation (17.28).

17.3.3.4 Increase in the Space–Time Yield at a Constant Ohmic Penalty

The combination of Equations (17.17) and (17.28) permits the attainable space–time yield in single-pass high-conversion reactors to be estimated:

$$\rho_{ST} \approx 2.69\frac{DM_B\overline{C_A^b}}{d^2} \tag{17.32}$$

Equation (17.32) shows that a decrease in the inter-electrode gap leads to the enhancement of the attainable space–time yield. *Moreover, for a given electrolyte conductivity, the process intensification is realized without enhancing the ohmic penalty,* as shown by the combination of Equations (17.11), (17.20) and (17.28):

$$\Delta\Phi_{ohm} \approx 2.69\frac{nFD\overline{C_A^b}}{\kappa} \tag{17.33}$$

17.3.3.5 Experimental Investigations Reported in the Literature

Several recent papers [6–12] have reported the use of microplate or microchannel cells for electro-organic synthesis purposes. The most important characteristics of these investigations are given in Table 17.1. The cell overall widths and lengths are in the centimeter range whereas the inter-electrode gap is between 25 and 320 μm. Various electrode materials are used: glassy carbon is often preferred for electro-organic oxidation reactions, whereas reductions are carried out on stainless-steel, platinum or nickel electrodes.

Different electro-organic reaction systems have been studied. The anodic reactions investigated are mainly the four-electron methoxylation of 4-methoxytoluene [6, 7, 11, 12] and the two-electron methoxylation of furan to 2,5-dimethoxy-2,5-dihydrofuran [10], but also other methoxylation and acetoxylation reactions [11]. Methoxylation reactions are performed in methanol as a solvent, whereas acetoxylations are performed in acetic acid. Moreover, Küpper *et al.* [7] reported the anodic two-electron decarboxylation of sodium glucanate in an aqueous medium. The cathodic

Table 17.1 Most important characteristics and results of recent literature investigations on electro-organic synthesis in micro-plate and microchannel reactors.

Reference	Reaction system(s) – electrode material – electrolyte composition		Cell dimensions:, SI units (m or m^2)	Operating conditions mentioned and evaluated using Equations (17.23) and (17.26) ($D = 10^{-9}\,m^2\,s^{-1}$)		Reactor performance (if mentioned)	
Löwe *et al.* [6]; Küpper *et al.* [7]	*Anode reactions*	**1**: methoxylation of 4-methoxytoluene; ($4e^-$)	27 parallel channels	C_A^{in}	10–200 mol m^{-3}	θ	**1**: 0.4–1
		2: decarboxylation of sodium glucanate	*channel dimensions:*	u	3.5×10^{-3}–8.3×10^{-2} m s^{-1}		**2**:–
	Anode material	glassy carbon	d 0.025×10^{-3}	i	200–800 A m^{-2}	ψ	**1**: 0.5–0.75
	Cathode reaction	hydrogen formation	w 0.8×10^{-3}	V	**1**: 4–10 V; **2**: –		**2**: 0.02–0.25
	Cathode material	stainless steel	L 64×10^{-3}	NTU	1.6–22	Φ	–
	Solvent:	**1**: methanol; **2**: water	*Overall electrode area given by authors*	I^*	0.17–7		
	Supp. electrolyte	**1**: KF 0.01 M or without; **2**: Na acetate	Ω 690×10^{-6}				
Paddon *et al.* [8]	*Anode reaction*	ethanol oxidation	d 0.1×10^{-3}	C_A^{in}	10–20 mol m^{-3}	θ	–
	Anode material	platinum	w 5×10^{-3}	u	6.3×10^{-5}–6.3×10^{-4} m s^{-1}	ψ	0.04–0.92
	Cathode reaction	reduction of tetraethyl ethylenetetracarboxylate ($2e^-$)	L 5×10^{-3}; 2.5×10^{-2}	i	8–60 A m^{-2}	Φ	–
			Ω 25×10^{-6}; 125×10^{-6}	V	3 V		
	Cathode material	nickel		NTU	2–106		
	Solvent	ethanol		I^*	1.2–19.6		
	Supp. electrolyte	$LiClO_4$ 0.1 M or without					

He *et al.* [9]	*Anode reaction*	?	d	0.16×10^{-3}; 0.32×10^{-3}	C_A^{in}	$10\,mol\,m^{-3}$	θ 0.58–100
	Anode material	platinum	w	3×10^{-3}	u	6.9×10^{-4}–$1.4\times10^{-3}\,m\,s^{-1}$	ψ 0.68–0.94
	Cathode reaction	reduction of 4-nitrobenzyl bromide ($1e^-$) leading to dimerization; reduction of the dimer ($1e^-$)	L	19×10^{-3}	i	$13–55\,A\,m^{-2}$	Φ 0.8 or less
			Overall electrode area given by authors		V	4–10 V	The reaction is self-propagating in the bulk
					NTU	0.56–2.27	
			Ω	45×10^{-6}	I^*	0.93–3.89	
	Cathode material	platinum					
	Solvent	DMF, DMF + THF					
	Supp. electrolyte	without					
Horii *et al.* [10, 11]	*Anode reactions*	methoxylation and acetoxylation of various aromatic substrates: furan; 4-methoxytoluene; 2,4,6-tri-*t*-butylphenol	d	0.08×10^{-3}	C_A^{in}	$10\,mol\,m^{-3}$	θ 0.15–1
			w	10×10^{-3}	Furan oxidation [10]:		ψ 0.10–0.98
			L	30×10^{-3}	u	2.1×10^{-4}–$2.1\times10^{-2}\,m\,s^{-1}$	Φ 10% or less
			Ω	300×10^{-6}	i	$1–100\,A\,m^{-2}$	
					V	7 V	
	Anode material	glassy carbon			*NTU*	1.2–120	
	Cathode reaction	hydrogen formation			I^*	0.3–93	
	Cathode material	platinum					
	Solvent	methanol, acetic acid					
	Supp. electrolyte	without					
Attour *et al.* [12]	*Anode reaction*	methoxylation of 4-methoxytoluene; ($4e^-$)	10	electrode segments in series	C_A^{in}	$10–100\,mol\,m^{-3}$	θ 0.05–1
	Anode material	glassy carbon	d	0.1×10^{-3}	u	1.7×10^{-3}–$2\times10^{-2}\,m\,s^{-1}$	ψ 0–0.8
	Cathode reaction	hydrogen formation	w	10×10^{-3}	i	$1–40\,A\,m^{-2}$	Φ 0.5–0.95
	Cathode material	stainless steel	L	10×10^{-3}	V	3–8 V	
	Solvent	methanol	*Overall electrode area*		*NTU*	1.3–16	
	Supp. electrolyte	KF 0.0025–0.1 M	Ω	1000×10^{-6}	I^*	0.1–2	

reactions discussed are the two-electron reduction of tetraethyl ethylenetetracarboxylate in ethanol [8] and the reduction of 4-nitrobenzyl bromide in DMF [9], which is a special reaction system, as the reaction is self-propagating in the bulk.

Most investigations, however, were performed under conditions which are not relevant for commercial production purposes [8–11]: dilute media (i.e. inlet reagent concentrations $\leq$0.02 M) and low average current densities (i.e. <100 A m^{-2}). Moreover, the selection of the operating conditions is empirical. In consequence, the number of transfer units [Equation (17.26)] and the dimensionless current [Equation (17.23)] are in an exceedingly wide range (see Table 17.1). Various research teams have nevertheless demonstrated the possibility of obtaining high reagent conversions together with high product selectivities, even in the absence of added supporting electrolyte [7–11]. *The different investigations thus clearly demonstrate the feasibility of and the interest in micro-structured single-pass high-conversion electro-organic synthesis cells.*

17.3.3.6 **Reactor Model**

Recently, our group developed and validated a reactor model suitable for design calculations in a thin-gap single-pass high-conversion electrochemical cell [23, 24]. The model is based on electrolyte plug flow and includes electrochemical kinetics and mass transfer limitations. It has been developed for the case of three consecutive electrochemical reactions, with the key product formed by the second reaction, but can easily be modified in order to be used for other reaction schemes, such as parallel reactions or solvent oxidation.

For given electrochemical kinetics, the reactor performance depends on only three independent dimensionless numbers: the dimensionless current [Equation (17.23)], *NTU* [Equation (17.26)] and a Wagner-like number which compares the kinetic resistance of the system with its ohmic resistance:

$$Wa = \frac{\kappa}{nFk_{\mathrm{m}}C_{\mathrm{A}}^{\mathrm{in}}\,\mathrm{d}b_{\mathrm{A}}} \tag{17.34}$$

Low Wagner numbers lead to uniform current density distributions over the electrode length, whereas high Wagner numbers induce uniform overpotential distributions.

The model simulations permit one to define optimum operating conditions for the single-pass high-conversion mode: a dimensionless current close to unity and *NTU* between 6 and 12, i.e. sufficiently high to permit the reagent to join the electrode surface. Highest selectivities and high current efficiencies are obtained when the Wagner number is high (*i.e.* $Wa > 0.5$), as the local current density adjusts to the decreasing reagent concentration. In the case of a natural uniform current density distribution (i.e. a low Wagner number), undesired reactions are favored at the reactor outlet, where the reagent concentrations are low. In this case, electrode segmentation may be used in order to force a decrease in the current-density over the electrode length [13].

The reactor model was validated successfully by measurements made in a thin-gap flow cell [24] with operating conditions close to those described in [12] and reported in Table 17.1. A serious difficulty encountered in experiments performed at relatively

high reagent inlet concentrations ($C_A^{in} = 0.1$ M) is related to the huge amount of electrogenerated hydrogen. As the gas phase is isolating versus electrical current, the conductivity in the inter-electrode gap decreases, leading to high cell voltages. This problem does not arise at low reagent concentrations, as the electrogenerated hydrogen remains dissolved in the electrolyte. The estimation of the gas and liquid fluxes as a function of the operating conditions is developed in [23].

17.4 Conclusion and Outlook

The reduction of the inter-electrode gap to the sub-millimeter scale clearly opens up new opportunities in the design of electrosynthesis cells. Process intensification is due to the thinning and the overlapping of the mass transfer boundary layers and also to the substantial decrease in the ohmic penalty, which are major concerns of electrochemical reaction engineering. Moreover, in the thin-gap cell, the high specific electrode area together with the high mass transfer rates permits the overall process scheme to be changed: single-pass high-conversion reactors can be envisioned.

The single-pass high-conversion reactor has proved feasible with dilute reagent concentrations [6–12]. However, if one of the electrode reactions involves gas evolution, a single-pass high-conversion mode of operating implies, under industrially relevant working conditions (i.e. high reagent inlet concentrations), very high gas production rates [23]. This phenomenon is detrimental to the current transport in the inter-electrode gap. An increase in the operating pressure would limit the amount of the volumetric gas flow under these conditions, but the feasibility of the electrochemical synthesis under these conditions should be demonstrated experimentally. Furthermore, only a few electrochemical syntheses have been realized so far in thin-gap high-conversion flow cells, whereas many industrially relevant simple or paired reaction systems could benefit from the coupling of the electrode processes [20]. Moreover, the conception and the construction of multilayer thin-gap cells permitting industrially relevant production rates to be reached and including eventually heat exchangers are still a technical challenge and there is clearly a lot of work to be done before micro-structured electrochemical cells can be introduced routinely in industrial processes.

List of Symbols

a_s	Specific electrode area (m^{-1})
A, B, C, D	Reagent or product of the electrochemical reaction
b_A	Kinetic constant of the reaction involving reagent A (V^{-1})
C_A	Concentration of reagent A ($mol\,m^{-3}$)
d	Inter-electrode gap (m)
D	Diffusion coefficient ($m\,s^{-1}$)
E^c, E^a	Cathodic, anodic potential (V)
E_e^c, E_e^a	Cathodic, anodic equilibrium potential (V)

E_{cell}	Cell voltage (V)
E_{tn}	Thermoneutral cell voltage (V)
F	Faraday constant (96 487 A s equiv^{-1})
i	Current density (A m^{-2})
I	Cell current (A)
I^*	Dimensionless cell current, defined by Equation (17.23)
k_A	Kinetic rate constant of the reaction involving reagent A (m s^{-1})
k_m	Mass transfer velocity (m s^{-1})
L	Electrode length (m)
M_B	Molar mass of product B (kg mol^{-1})
n, n'	Number of electrons involved (equiv mol^{-1})
$\dot{n}$	Molar flux (mol s^{-1})
NTU	Number of transfer units, defined by Equation (17.26)
Q_L	Electrolyte volumetric flow rate (m^3 s^{-1})
Q_{mol}	Electric charge required per mole of reagent (A s)
Q_{Joule}	Heat generation flux (W)
R_{cell}	Equivalent electrical cell resistance (Ω)
$R_{circuit}$	Equivalent resistance of the electrical circuit (Ω)
Re	Reynolds number, Equation (17.27)
Sc	Schmidt number, Equation (17.27)
Sh	Sherwood number, Equation (17.27)
u_L	Superficial velocity of the liquid phase, $u_L = Q_L/(dw)$ (m s^{-1})
V	Cell voltage (V)
V_R	Reactor volume (mL)
w	Electrode width (m)
Wa	Wagner number, defined by Equation (17.34)
x	Spatial coordinate

Greek Letters

$\Delta\Phi_{ohm}$	Ohmic resistance of the cell
Φ	Current efficiency
η^a, η^c	Anodic, cathodic overpotential (V)
κ	Electrolyte conductivity (S m^{-1})
θ	Reagent conversion
ρ_{st}	Space–time yield
σ	Selectivity versus the desired product
ψ	Product yield
Ω	Electrode area, $\Omega = Lw$ (m^2)

Suffixes

—	Space averaged value
in	Relative to the reactor inlet
out	Relative to the reactor outlet

Subscripts

b	Relative to the bulk
i	Relative to the liquid–solid interface
lim	Limiting value

References

1 H. Pütter, in *Organic Electrochemistry*, 4th edn, ed. H. Lund, O. Hammerich, Marcel Dekker, New York, **2001**, Chapter 31.

2 D. Pletcher, F. C. Walsh, *Industrial Electrochemistry*, 2nd edn, Chapman and Hall, London, **1990**.

3 K. Jüttner, in *Encyclopedia of Electrochemistry, Vol. 5. Electrochemical Engineering*, ed. D. D. Macdonald, P. Schmucki, Wiley-VCH Verlag GmbH, Weinheim, **2007**, Chapter 1.

4 F. Beck, H. Goldacker, G. Kreysa, H. Vogt, H. Wendt, in *Ullmann's Encyclopedia of Industrial Chemistry, Vol. A9, Electrochemistry*, 5th edn, **1990**, VCH Verlag GmbH, Weinheim.

5 F. Coeuret, A. Storck, *Eléments de Génie Electrochimique*, Techniques et Documentations, Lavoisier, Paris, **1985**.

6 H. Löwe, M. Küpper, A. Ziogas, Reactor and method for carrying out electrochemical reactions, patent number, WO 0015872, DE 19841302, **2002**.

7 M. Küpper, V. Hessel, H. Löwe, W. Stark, J. Kinkel, M. Michel, H. Schmidt-Traub, Micro reactor for electroorganic synthesis in the simulated moving bed-reaction and separation environment, *Electrochim. Acta*, **2003**, *48*, 2889–2896.

8 C. A. Paddon, G. J. Pritchard, T. Thiemann, F. Marken, Paired electrosynthesis: micro-flow cell processes with and without added electrolyte, *Electrochem. Commun.*, **2002**, *4*, 825–831.

9 P. He, P. Watts, F. Marken, S. J. Haswell, Electrolyte free electro-organic synthesis: the cathodic dimerization of 4-nitrobenzyl bromide in a micro-gap flow cell, *Electrochem. Commun.*, **2005**, *7*, 918–924.

10 D. Horii, M. Atobe, T. Fuchigami, F. Marken, Self-supported paired electrosynthesis of 2,5-dimethoxy-2,5-dihydrofuran using a thin layer flow cell without intentionally added supporting electrolyte, *Electrochem. Commun.*, **2005**, *7*, 35–39.

11 D. Horii, M. Atobe, T. Fuchigami, F. Marken, Self-supported methoxylation and acetoxylation electrosynthesis using a simple thin-layer flow cell, *J. Electrochem. Soc.*, **2006**, *153*, D143–D147.

12 A. Attour, S. Rode, A. Ziogas, M. Matlosz, F. Lapicque, A thin-gap cell for selective oxidation of 4-methylanisole to 4-methoxybenzaldehyde dimethylacetal, *J. Appl. Electrochem.*, **2008**, *38*, 339–347.

13 S. Rode, S. Altmeyer, M. Matlosz, Segmented thin-gap flow cells for processintensification in electrosynthesis, *J. Appl. Electrochem.*, **2004**, *34*, 671–680.

14 C. Belmont, H. H. Girault, Coplanar interdigitated band electrodes for synthesis Part 1. Ohmic loss evaluation, *J. Appl. Electrochem.*, **1994**, *24*, 475–480.

15 C. Belmont, H. H. Girault, Coplanar interdigitated band electrodes for electrosynthesis Part 2. Methoxylation of furan, *J. Appl. Electrochem.*, **1994**, *24*, 719–724.

16 C. Belmont, H. H. Girault, Coplanar interdigitated band electrodes for electrosynthesis. Part 3. Epoxidation of propylene, *Electrochim. Acta*, **1995**, *40*, 2505–2510.

17 C. Belmont, R. Ferrigno, O. Leclerc, H. H. Girault, Coplanar interdigitated band electrodes for electrosynthesis. Part 4. Application to sea water electrolysis, *Electrochim. Acta*, **1998**, *44*, 597–603.

18 R. Ferrigno, J. Josserand, V, P. F. Brevet, H. H. Girault, Coplanar interdigitated band electrodes for electrosynthesis. Part 5. Finite element simulation of paired reactions, *Electrochim. Acta*, **1998**, *44*, 587–595.

19 R. Ferrigno, C. Comninellis, V. Reid, C. Modes, R. Scannell, H. H. Girault, Coplanar interdigitated band electrodes for electrosynthesis. Part 6. Hypochlorite electrogeneration from sea water electrolysis, *Electrochim. Acta*, **1999**, *44*, 2871–2878.

20 C. A. Paddon, M. Atobe, T. Fuchigali, P. He, P. Watts, S. J. Haswell, G. J. Prichard, S. D. Bull, F. Marken, Towards paired and coupled electrode reactions for clean organic microreactor electrosyntheses, *Appl. Electrochem.*, **2006**, *36*, 617–634.

21 D. J. Pickett, *Electrochemical Reactor Design*, 2nd edn, Elsevier, Amsterdam, **1979**, Chapter 4.

22 W. J. Beek, K. M. K. Muttzall, J. W. van Heuven, *Transport Phenomena*, 2nd edn, John Wiley and Sons, Ltd, Chichester, **1999**, Chapter 3.

23 S. Rode, A. Attour, F. Lapicque, M. Matlosz, A thin-gap single-pass high conversion reactor for organic electrosynthesis. Part I: model development, *J. Electrochem. Soc.*, **2008**, *155*, E193–E200.

24 A. Attour, S. Rode, F. Lapicque, A. Ziogas, M. Matlosz, A thin-gap single-pass high conversion reactor for organic electrosynthesis. Part II: application to the methoxylation of 4-methoxytoluene, *J. Electrochem. Soc.*, **2008**, *155*, E201–E206.